Using Temperature Signals to Estimate Geometry Parameters in Fractured Geothermal Reservoirs

F. Maier[1], P. Oberdorfer[1], I. Kocabas[2], I. Ghergut[1], M. Sauter[1]
[1]University of Göttingen, Germany, [2]Batman University, Turkey
*Corresponding author: 37077 Göttingen, Goldschmidstr. 3, fmaier@gwdg.de

Abstract: For this study we use COMSOL Multiphysics 4.2a and the Subsurface Flow Module. We compare the output of 2D single fracture models as well as analytical solutions (Kocabas 2010) of the problem. The temperature signal is evaluated with the heat transfer mode while the coupled flow field is assumed to exhibit Darcy flow everywhere. The problem is time-dependent so we have to take into account a change in the boundary conditions from a Dirichlet to a Neumann condition which is activated at the time of change from the injection to the withdrawal phase. A numerical dispersion problem is encountered at the abrupt temperature change at the thermal front. The resolution in time and space of this step is the numerical "bottleneck" of the problem. Depending on the cell Peclet number we obtain an increasing/decreasing accuracy due to numerical dispersion. In case of high accuracy the solutions show negligible deviations.

Keywords: SWIW, thermal injection-backflow tests, COMSOL Subsurface Module, simulation of temperature transients (signals), numerical dispersion.

1. Introduction

Geothermal energy is considered to be a major potential source for energy supply in the currently ongoing turnover. The resource is stored in deep (3 – 5 km) subsurface reservoirs. To estimate efficiency of geothermal energy recovery knowledge of reservoir characteristics and thermal transport parameters is a prerequisite. Tracer testing have been widely used determine reservoir parameters. Here, tracer is a substance or energy quantity with known physical and/or chemical behavior, e.g. dyes, heat, radioactive isotopes. In general the tracer is injected into the reservoir, interacts with the reservoir material and is finally abstracted again. In tracer tests, state variables such as concentrations or temperature are monitored to obtain the return profiles and interpreted to infer estimates of transport parameters. Recently, heat has emerged as a useful type of tracer in which thermal transients have been monitored and temperature is employed as the state variable. The temperature return profile is analyzed to identify the equivalent fracture width or more precisely heat transport rate in a fracture/matrix configuration. There are several ways of performing a tracer test. In this study we focus on Single-Well Thermal Injection-Withdrawal Experiments (SWTIW), also known as Push-Pull Experiments, in a single fracture located in a low permeability matrix. The experimental design has two phases. Phase one starts with the injection of fluid with a defined temperature. In phase two we immediately abstract the fluid and record the temperature at the abstraction point. The analysis aims at the identification of the equivalent fracture width embedded in a dimensionless heat transfer rate parameter and this information can be obtained just from this temperature signal.

2. Use of COMSOL Multiphysics

In the presented study COMSOL Multiphysics 4.2a is used. For the time dependent study we apply the physics interfaces called as 'Heat Transfer in Porous Media' and

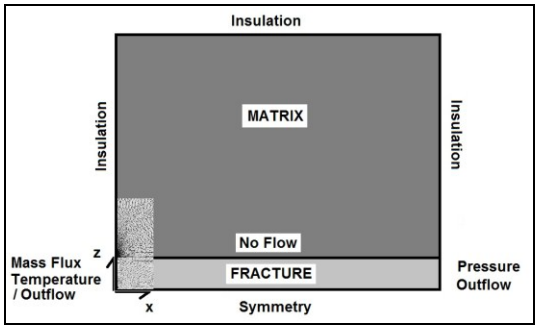

Figure 1. Sketch of the model domain with hydraulic and thermal boundary conditions. The 'Mass Flux' and hence the advective heat flux changes sign after the injection phase. For the thermal boundary we then have a transition in the boundary condition from Dirichlet to Neumann (Maier et al. 2011).

'Darcy's Law' which are part of the 'Subsurface Flow Module'. The two interfaces couple the steady fluid flow and the unsteady heat transport fields quite effectively. The model domain consists of two subdomains, the fracture and the adjacent matrix (Fig. 1).

Within that fracture/matrix geological configuration we assume an infinite lateral thermal conductivity in the fracture whereas the heat conduction and dispersion in the flow direction is neglected. In the matrix we assume a constant thermal conductivity. Thus the governing equations during the injection period reads:

$$\rho_f c_f \frac{\partial T}{\partial t} + \rho_w c_w \phi u \frac{\partial T}{\partial x} - \frac{k_m}{b}\frac{\partial T_m}{\partial z}\Big]_{z=0} = 0 \qquad (1)$$

$$\rho_m c_m \frac{\partial T_m}{\partial t} - k_m \frac{\partial^2 T_m}{\partial z^2} = 0 \qquad (2)$$

Here the origin is shifted to the fracture matrix boundary. The concerning initial and boundary conditions are given by:

$$T = T_m = T_0 \quad \text{at} \quad t = 0 \qquad (3)$$

$$T = T_i \quad \text{at} \quad x = 0 \qquad (4)$$

$$T = T_m \quad \text{at} \quad z = 0 \qquad (5)$$

$$T_m \to 0 \quad \text{as} \quad z \to \infty \qquad (6)$$

For the backflow period, equations 2, 5 and 6 remains the same. The others changes as follows:

$$\rho_f c_f \frac{\partial T}{\partial t_p} - \rho_w c_w \phi u \frac{\partial T}{\partial x} - \frac{k_m}{b}\frac{\partial T_m}{\partial z}\Big]_{z=0} = 0 \qquad (7)$$

$$T = T(t_p = 0) \quad \text{at} \quad t_p = 0 \qquad (8)$$

$$T = T_i \quad \text{at} \quad x = L = u t_j \qquad (8)$$

$$T_m = T_m(t_p = 0) \quad \text{at} \quad t_p = 0 \qquad (9)$$

Where t_j is the total injection time and t_p is the time variable for the backflow period.

2.1 Governing Equations

To implement the given mathematical model in COMSOL Multiphysics we solve for the steady flow field in the fracture using Darcy´s Law:

$$u = \frac{-K}{\rho_w g}\nabla p \qquad (10)$$

The fluid flow solution is coupled into the Advection-Dispersion-Equation of the heat transport, which is solved everywhere:

$$\rho c \frac{\partial T}{\partial t} + \rho c u \cdot \nabla T = \nabla \cdot (k \nabla T) \qquad (11)$$

with

$$\rho c = (1-\phi)\rho_R c_R + \phi \rho_W c_W \qquad (12)$$

and

$$k = (1-\phi)\begin{pmatrix} k_R & 0 \\ 0 & 0 \end{pmatrix} + \phi \begin{pmatrix} k_W & 0 \\ 0 & 0 \end{pmatrix}. \qquad (13)$$

The porosity ϕ is space dependent with $\phi = .5$ inside of the fracture and zero in the matrix. Hence we have solely heat conduction in the matrix. For the thermal conductivity k we need to meet the requirement of the system of equations given above the lateral thermal conductivity inside of the fracture is chosen to be $k_f = 1000 * k$. (14)

2.2 Numerical Model

To save computational power the model domain is automatically adjusted to the region of interest. The fracture length is two times the travel distance of the tracer to avoid bias due to boundary effects. The travel distance is calculated from the Darcy velocity. While the width of the adjacent matrix is automatically calculated to five times the travel distance. At the inlet we apply a boundary layer to account for the injected abrupt temperature change (Fig. 2). This change is the numerical "bottleneck". Since a vanishing dipersivity, which we assume for

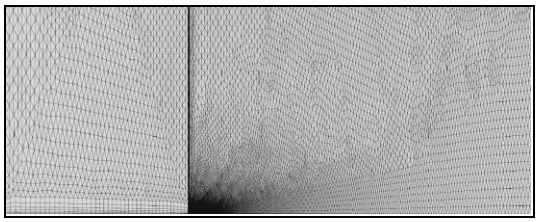

Figure 2. Zoom of the boundary layer/free triangular mesh. The boundary layers are at the inlet and at the fracture/matrix boundary on the matrix side.

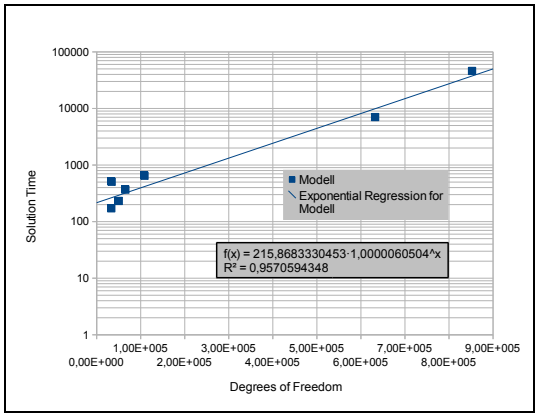

Figure 3. The models were solved on an Intel(R) Core(TM) i7 CPU, Q 820 @1.73GHz, 8 GB RAM, 64-bit Windows 7 system

our model, leads to high cell Peclet number:

$$Pe_{cell} = \frac{\Delta l}{\alpha} \tag{15}$$

Where α is the dispersivity. Hence we have to apply a very fine mesh to minimize the cell Peclet number and to resolve the abrupt temperature change by minimizing the numerical dispersion. In theory this is possible, but unfortunately the increasing number of elements/degrees of freedom leads to unreasonable long computational times (Fig. 3). . For our model we obtain a exponential increase in computational time with increasing degrees of freedom.

To estimate the effect of numerical dispersion on the recorded temperature signal we compare the numerical with analytical results of the described problem.

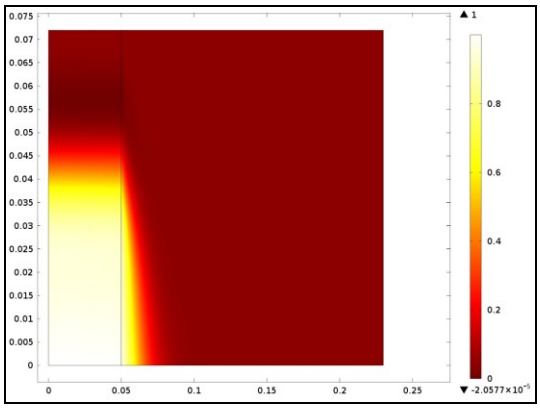

Figure 4. Temperature distribution in the model domain after the injection for $\alpha = 0.036$.

3. Results

The given mathematical model (Eq. 1 through Eq. 9) of the problem can be solved via iterated Laplace transforms. A detailed derivation can be found in Kocabas (2010). The Solution for the dimensionless temperature T_D is given by:

$$T_D = \int_0^{\min(1,\frac{t_n}{\lambda})} \frac{\exp\left(-\frac{\lambda^2\alpha\omega^2}{4(t_n-\lambda\omega)}\right)}{\sqrt{\pi(t_n-\lambda\omega)}}\, d\omega + \operatorname{erfc}\left(\frac{\sqrt{\alpha}\,\omega}{2\sqrt{(1-\omega)}}\right)\left(\frac{\lambda^2\sqrt{\alpha}\,\omega}{2(t_n-\lambda\omega)}+\lambda\sqrt{\alpha}\right)$$

$$\int_0^1 \int_0^{\min\left(1-\eta,\frac{t_n+\eta}{\lambda}\right)} \frac{\exp\left(\frac{-\alpha\omega^2}{4(1-\eta-\omega)}\right)}{\sqrt{\pi(1-\eta-\omega)}} \frac{\exp\left(\frac{-\lambda^2\alpha\omega^2}{4(t_n+\eta-\lambda\omega)}\right)}{2\sqrt{\pi(t_n+\eta-\lambda\omega)}} \left(\frac{\lambda^2\alpha\omega}{t_n+\eta-\lambda\omega}-\frac{\lambda\alpha\omega}{1-\eta-\omega}\right) d\omega d\eta \tag{16}$$

Where t_n is the dimensionless pumping time, η and ω are the dummy variables of the iterated Laplace transformation, λ is the ratio of the injection-/pumping rate which is equated to one for all of the presented models and α is the dimensionless heat transfer rate parameter which is given by

$$\alpha = \frac{\rho_R c_R k}{(\rho c)^2}\frac{t_i}{b^2}. \tag{17}$$

For a unit value of the parameter α we can see that the Temperature at the outlet is independent of the flow velocity. Therefore we can choose an arbitrary pumping rate and porosity to meet a good solvability of the numerical models. In a given geological configurations the first fraction is fixed, while the second fraction contains the injection time t_i

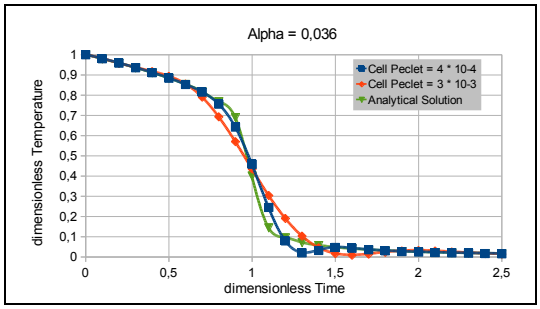

Figure 5. Temperature signal at the outlet during the withdrawal phase.

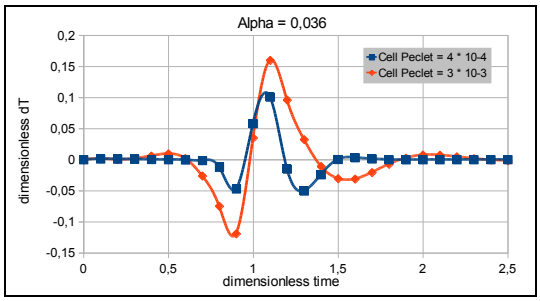

Figure 6. Deviation of the numerical results from the analytical solution.

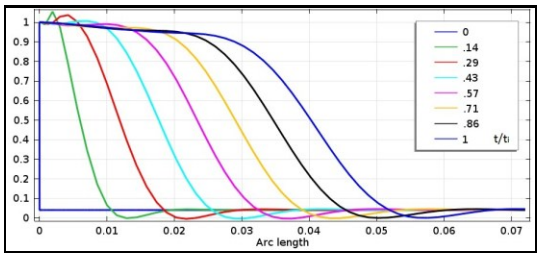

Figure 7. Temperature distribution along the fracture for different time steps while injecting. Here α is 0.036 and the cell Peclet number is $3 * 10^{-3}$.

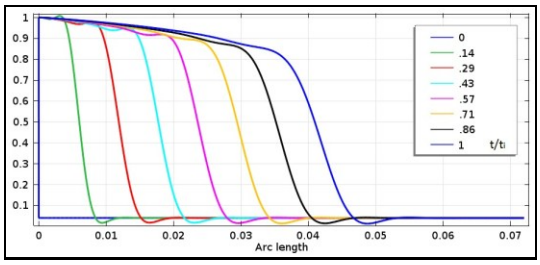

Figure 8. Temperature distribution along the fracture for different time steps while injecting. Here α is 0.036 and the cell Peclet number is $4 * 10^{-4}$.

and the target parameter: the fracture half width b.

The advancing front of the abrupt temperature change in the fracture is accompanied with a temperature signal which diffuse into the adjacent matrix (Fig. 4). In dependence of the heat transfer rate parameter we obtain for decreasing α values a decreasing fracture/matrix heat exchange. This effect is visible in Figure 5 where we obtain an almost conserved temperature signal height for early data points (t<1). The comparison with the analytical results shows that the deviation decrease with a decreasing cell Peclet number (Fig. 6) and for lower cell Peclet numbers less data points are biased.

The bias is due to numerical dispersion which leads to oscillations and a smearing of the advancing front (Fig. 7 and Fig. 8). Hence the bias starts earlier for higher cell Peclet numbers and last longer. The highest deviations occur in the region when the pumping time equals the injection time, in other words when the injected front reaches the inlet again. The lower cell Peclet number (Fig. 8) shows less oscillations and a steeper thermal front.

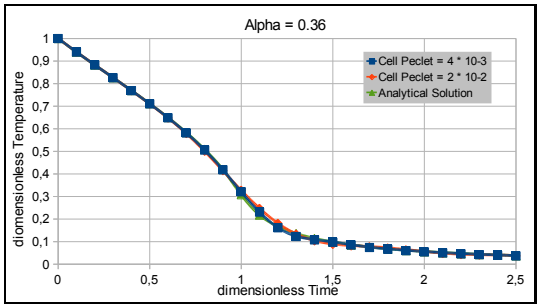

Figure 9. Temperature signal at the outlet during the withdrawal phase.

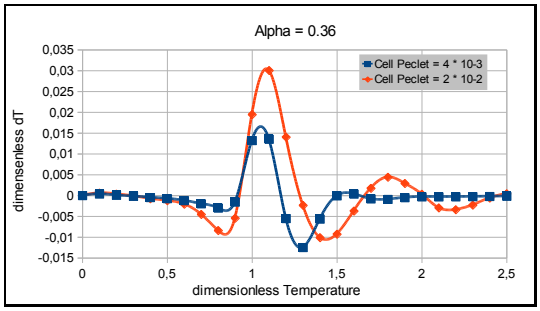

Figure 10. Deviation of the numerical results from the analytical solution.

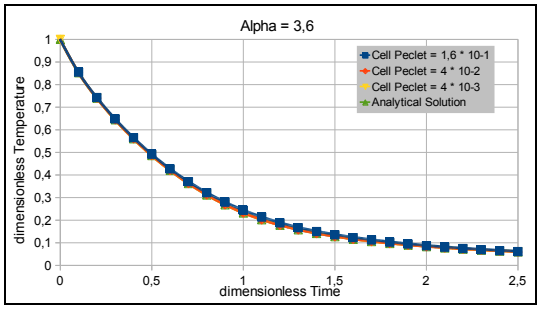

Figure 11. Temperature signal at the outlet during the withdrawal phase.

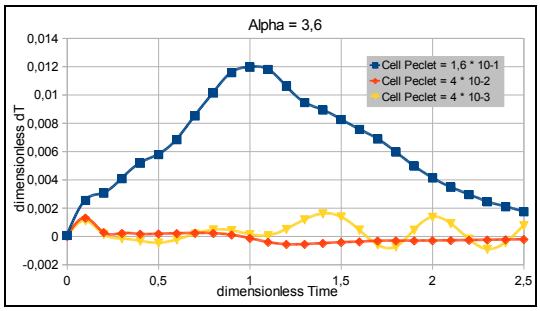

Figure 12. Deviation of the numerical results from the analytical solution.

For increasing α the influence of the numerical dispersion on the temperature signal reduce in magnitude but has the same shape (Fig. 9 and Fig. 10). Hence less effort has to be taken to get reasonable results. This behavior is due to the amount of heat which is transferred into the matrix. For higher α values more heat is exchanged which leads to a decaying thermal front. Therefore we obtain a minimizing of the error made due to numerical dispersion which affects the front most heavily.

The influence of the numerical dispersion becomes negligible for $\alpha > 1$. This is shown in Figure 11 for $\alpha = 3.6$. While the effect of numerical dispersion vanished for high α values it is still not possible to use a too coarse mesh because this leads to a underestimation of the transferred heat and therefore to a biased temperature signal were the signal obtained from the numerical simulation is too high (Fig. 12).

4. Discussion and Conclusion

The modeling of discontinuous functions is a great challenge in numerical FE modeling. The neglected diffusion/dispersion in flow direction is a benchmark to estimate the influence of numerical dispersion on the results. On the other hand the comparison of the numerical results with the analytical solution allows the identification of critical zones in the recorded temperature signal, which deviate due to diffusion/dispersion. Depending on the cell Peclet number and α one can see that with a smaller cell Peclet number the biased range gets also smaller as well as the magnitude of the deviation. In the considered data range we obtain that for each order of magnitude of increasing α the deviation for a given cell Peclet number (here $4 * 10^{-3}$) decrease by one order of magnitude. In general the numerical dispersion problem is encountered at the abrupt temperature change at the thermal front. The resolution in time and space of this step is the numerical "bottleneck" of the problem.

Summarized we have to decide between the solution time and deviation due to a too coarse grid. For lower α values we have to consider the error due to numerical dispersion since a greater amount of data points are affected. On the other hand for high α values, where numerical dispersion is negligible, we are not able to apply a too coarse mesh, because this leads to an overestimation of the resulted temperature.

5. References

1. Kocabas, I.. “Designing Thermal and Tracer Injection Backflow Tests.” *World* C.2010: 25-29. (2010)
2. Maier F., Hebig K, Jin Y. and Holzbecher E.: Ability of Single-Well Injection-Withdrawal Experiments to Estimate Ground Water Velocity. In: Proceedings of COMSOL Conference 2011 (Stuttgart), CD-ROM-Publication (2011)

6. Acknowledgements

This work acknowledge financial support from the German Ministry for Environment (BMU) and the EnBW within project “LOGRO” under grant no. 0325111B, for the opportunity of conducting numerical and field SWIW tracer tests aimed at characterizing deep-sedimentary geothermal reservoirs in Germany.